J. Quant. Spectrosc. Radiat. Transfer. Vol. 11, pp. 1441–1462. Pergamon Press 1971. Printed in Great Britain

NON-GREY RADIATIVE HEAT TRANSFER IN CONSERVATIVE PLANE-PARALLEL MEDIA WITH REFLECTING BOUNDARIES

R. J. REITH, JR., C. E. SIEWERT and M. N. ÖZIŞIK

Departments of Nuclear and Mechanical Engineering, North Carolina State University, Raleigh, N.C. 27607, U.S.A.

(*Received* 23 *November* 1970)

Abstract—The normal-mode-expansion technique is used to solve a class of non-grey radiative heat transfer problems in finite plane-parallel media appropriate to radiative and local thermodynamic equilibrium conditions. The frequency-dependent absorption coefficient is characterized by a two-band 'picket-fence' model. The boundary surfaces are maintained at uniform, but arbitrary, temperatures and are allowed to be diffuse emitters of radiant energy and to possess both specular and diffuse components of reflectivity. Rigorous solutions of the vector equation of transfer are constrained to meet the considered boundary conditions, and pertinent orthogonality relations are invoked to convert the resulting singular integral equations to coupled non-singular integral equations. All relevant integrals are represented by a high-order Gaussian-quadrature scheme, and the system of regular integral equations is solved iteratively to yield sufficiently accurate solutions for the required expansion coefficients. In addition to being used to evaluate the accuracy of developed, tractable analytical approximations, these 'exact' expansion coefficients render available the complete angular intensity of radiation at any optical depth in the medium. To report a parameter survey tabular results are given for the temperature-profile and heat-flux functions for a representative class of cases.

1. INTRODUCTION

THE picket-fence model as an approximation to non-grey radiative transfer has been discussed in two early papers by CHANDRASEKHAR[1] and MÜNCH.[2] The fact that the absorption coefficient is represented by a set of discrete values, rather than a single value, is basic to the picket-fence model, and thus the effects of resonance lines are included in the formulation of the equation of radiative transfer. As one of the first astrophysical applications of this model, CHANDRASEKHAR[1] has reported a diffusion-theory solution of the classical Milne problem, and more recently BOND and SIEWERT[3] numerically evaluated the exact analytical solution[4] of the Milne problem.

With the emphasis directed more explicitly toward engineering applications, LICK[5] and GREIF[6] have discussed the picket-fence model in connection with a study of combined radiative and conductive heat transfer; however, because of the complexity of the equations involved, only approximate analytical methods were used. The most elegant and rigorous work on the engineering aspects of this non-grey heat transfer model is that of SIMMONS and FERZIGER[7] who used the normal modes[4] of the equation of transfer as a basis for numerical calculations in finite plane-parallel media. Though the work of SIMMONS and FERZIGER[7] represents the first semi-analytical treatment of finite-slab problems

appropriate to the picket-fence model, they consider only the case of black boundaries and do not attempt to report calculations of bench mark accuracy.

In the present paper, we report the required extension of the analysis of finite-slab problems, defined in terms of the picket-fence model, to include the effects of specularly and diffusely reflecting boundaries. We cast our analysis in the familiar H-function notation of CHANDRASEKHAR[8], and we illustrate that computations relevant to the considered model can be made with a suitably high degree of precision. Further, we present the results of a rather extensive parameter survey and investigate several approximations to the 'exact' solution.

Since the picket-fence model to non-grey theory has been reviewed recently by SIMMONS and FERZIGER,[7] we give here only a brief sketch of the formulating equations. We consider the equation of transfer

$$\mu\frac{\partial}{\partial z}I_\nu(z,\mu) + \rho(z)k_\nu I_\nu(z,\mu) = \rho(z)k_\nu B_\nu[T(z)], \tag{1}$$

where $I_\nu(z,\mu)$ is the radiation intensity, considered as a function of the frequency ν, the position z, and the direction cosine μ (measured from the positive z-axis) of the propagating radiation. Further, $\rho(z)$ denotes the density of the medium, k_ν is the frequency-dependent absorption coefficient, and $B_\nu[T(z)]$ is the Planck black-body function:

$$B_\nu[T(z)] = \frac{2h\nu^3}{c^2}\left[\exp\left(\frac{h\nu}{kT(z)}\right) - 1\right]^{-1}. \tag{2}$$

We now consider that the entire frequency spectrum is divided into two (uniform or non-uniform) bands $\Delta\nu_1$ and $\Delta\nu_2$ such that the radiative properties are constant in the two regions. Denoting the two constant values of k_ν by k_1, $\nu\in\Delta\nu_1$, and k_2, $\nu\in\Delta\nu_2$, we integrate equation (1) to find

$$\mu\frac{\partial}{\partial\tau}\mathbf{I}(\tau,\mu) + \boldsymbol{\Sigma}\mathbf{I}(\tau,\mu) = \mathbf{C}\int_{-1}^{1}\mathbf{I}(\tau,\mu')\,d\mu', \tag{3}$$

where the condition of radiative equilibrium,

$$\int_0^\infty k_\nu B_\nu[T(z)]\,d\nu = \frac{1}{2}\int_0^\infty k_\nu\int_{-1}^{1} I_\nu(z,\mu)\,d\mu\,d\nu, \tag{4}$$

has been used. Here $\mathbf{I}(\tau,\mu)$ is a two-vector with elements $I_i(\tau,\mu)$ defined by

$$I_i(\tau,\mu) = \int_{\Delta\nu_i} I_\nu(\tau,\mu)\,d\nu, \qquad i = 1 \text{ or } 2, \tag{5}$$

and τ is the optical variable defined in terms of the smaller of the two values of the absorption coefficient (assumed without loss of generality to be k_2):

$$d\tau = \rho(z)k_2\,dz. \tag{6}$$

Further, in writing equation (3), we have defined the removal matrix as

$$\boldsymbol{\Sigma} = \begin{vmatrix}\sigma & 0\\ 0 & 1\end{vmatrix}, \sigma = \frac{k_1}{k_2} > 1, \tag{7a}$$

and the transfer matrix as

$$\mathbf{C} = \frac{1}{2(\sigma w_1 + w_2)} \begin{vmatrix} \sigma^2 w_1 & \sigma w_1 \\ \sigma w_2 & w_2 \end{vmatrix}, \tag{7b}$$

where w_1 and w_2 are given by

$$w_i = \frac{\pi}{\bar{\sigma} T^4(z)} \int_{\Delta\nu_i} B_\nu[T(z)]\, \mathrm{d}\nu, \qquad i = 1 \text{ or } 2, \tag{8}$$

with $\bar{\sigma}$ denoting the Stefan–Boltzmann constant and $T(z)$ the local temperature. Clearly w_1 and w_2 must sum to unity.

Seeking solutions in the medium bounded by parallel planes at $z = 0$ and $z = z_0$, we consider frequency-dependent boundary conditions of the form

$$I_\nu(0, \mu) = \varepsilon_{1\nu} B_\nu[T_1] + \rho^s_{1\nu} I_\nu(0, -\mu) + 2\rho^d_{1\nu} \int_0^1 I_\nu(0, -\mu')\mu'\, \mathrm{d}\mu', \qquad \mu \in (0, 1), \tag{9a}$$

and

$$I_\nu(z_0, -\mu) = \varepsilon_{2\nu} B_\nu[T_2] + \rho^s_{2\nu} I_\nu(z_0, \mu) + 2\rho^d_{2\nu} \int_0^1 I_\nu(z_0, \mu')\mu'\, \mathrm{d}\mu', \qquad \mu \in (0, 1). \tag{9b}$$

Here T_α, $\varepsilon_{\alpha\nu}$, $\rho^s_{\alpha\nu}$ and $\rho^d_{\alpha\nu}$, $\alpha = 1$ or 2, are respectively the temperature, emissivity, specular reflectivity and diffuse reflectivity at the boundary surfaces $z = 0\,(\alpha = 1)$ and $z = z_0\,(\alpha = 2)$.

Consistent with the considered two-band model, we now assume (as was assumed for the absorption coefficient k_ν) that the emissivity and reflectivity also have two values; we thus integrate equations (9) over the frequency ranges $\Delta\nu_i$, $i = 1$ and 2, to find the required boundary conditions on the two-vector $\mathbf{I}(\tau, \mu)$:

$$\mathbf{I}(0, \mu) = \mathbf{A}_1 + \mathbf{B}^s_1 \mathbf{I}(0, -\mu) + 2\mathbf{B}^d_1 \int_0^1 \mathbf{I}(0, -\mu')\mu'\, \mathrm{d}\mu', \qquad \mu \in (0, 1), \tag{10a}$$

and

$$\mathbf{I}(\tau_0, -\mu) = \mathbf{A}_2 + \mathbf{B}^s_2 \mathbf{I}(\tau_0, \mu) + 2\mathbf{B}^d_2 \int_0^1 \mathbf{I}(\tau_0, \mu')\mu'\, \mathrm{d}\mu', \qquad \mu \in (0, 1). \tag{10b}$$

Here τ_0 is the optical thickness of the slab and $\mathbf{A}_\alpha$, $\mathbf{B}^s_\alpha$, and $\mathbf{B}^d_\alpha$, $\alpha = 1$ or 2, are known constants defined in terms of previously mentioned quantities:

$$\mathbf{A}_\alpha = \frac{\bar{\sigma}}{\pi} T^4_\alpha \begin{vmatrix} \varepsilon_{\alpha 1} & w_1 \\ \varepsilon_{\alpha 2} & w_2 \end{vmatrix} \tag{11a}$$

and

$$\mathbf{B}^i_\alpha = \begin{vmatrix} \rho^i_{\alpha 1} & 0 \\ 0 & \rho^i_{\alpha 2} \end{vmatrix}, \quad \alpha = 1 \text{ or } 2,\ i = s \text{ or } d. \tag{11b}$$

With the foregoing definitions introduced, we proceed to construct a solution to the considered equation of transfer, equation (3), constrained to satisfy the boundary conditions given by equations (10).

2. GENERAL ANALYSIS

Since the normal modes for the equation of transfer have been established,[4] we write the general solution to equation (3) as

$$\mathbf{I}(\tau,\mu) = A_+\mathbf{I}_+ + A_-\mathbf{I}_-(\tau,\mu) + \int_{-1/\sigma}^{1/\sigma} A_1(\eta)\mathbf{\Phi}_1(\eta,\mu)\,e^{-\tau/\eta}\,d\eta + \int_{-1}^{1} A(\eta)\mathbf{\Phi}(\eta,\mu)\,e^{-\tau/\eta}\,d\eta, \quad (12)$$

where

$$\mathbf{I}_+ = \begin{vmatrix} \frac{1}{\sigma}c_{12} \\ c_{22} \end{vmatrix}, \qquad \mathbf{I}_-(\tau,\mu) = \begin{vmatrix} \frac{1}{\sigma}c_{12}(\tau - \mu/\sigma) \\ c_{22}(\tau - \mu) \end{vmatrix}, \quad (13a, b)$$

$$\mathbf{\Phi}_1(\eta,\mu) = \begin{vmatrix} c_{12}\delta(\sigma\eta - \mu) \\ -c_{11}\delta(\eta - \mu) \end{vmatrix}, \qquad \eta \in (-1/\sigma, 1/\sigma), \quad (13c)$$

and

$$\mathbf{\Phi}(\eta,\mu) = \mathbf{\Phi}_2(\eta,\mu)\Theta(\eta) + \mathbf{\Phi}_3(\eta,\mu)[1 - \Theta(\eta)]. \quad (13d)$$

Here we have written $\mathbf{\Phi}(\eta,\mu)$ as a sum of the vectors

$$\mathbf{\Phi}_2(\eta,\mu) = \begin{vmatrix} c_{12}\eta\dfrac{P}{\sigma\eta - \mu} + \delta(\sigma\eta - \mu)[-2\eta c_{12}\mathcal{T}(\sigma\eta)] \\ c_{22}\eta\dfrac{P}{\eta - \mu} + \delta(\eta - \mu)[1 - 2\eta c_{22}\mathcal{T}(\eta)] \end{vmatrix}, \qquad \eta \in (-1/\sigma, 1/\sigma), \quad (14a)$$

and

$$\mathbf{\Phi}_3(\eta,\mu) = \begin{vmatrix} c_{12}\eta\dfrac{1}{\sigma\eta - \mu} \\ c_{22}\eta\dfrac{P}{\eta - \mu} + \delta(\eta - \mu)\left[1 - 2\eta c_{11}\mathcal{T}\left(\dfrac{1}{\sigma\eta}\right) - 2\eta c_{22}\mathcal{T}(\eta)\right] \end{vmatrix}, \quad (14b)$$

$-1, -1/\sigma$ and $1/\sigma, 1$,

by utilizing the definition

$$\begin{aligned} \Theta(\eta) &= 1, \quad \eta \in (-1/\sigma, 1/\sigma), \\ &= 0, \quad \text{otherwise.} \end{aligned} \quad (15)$$

In addition, the symbol P is used in the above equations to indicate that all ensuing integrals over η or μ are to be evaluated in the Cauchy principal-value sense, the Dirac delta function is written as $\delta(x)$ and, for the sake of brevity, the abbreviation $\mathcal{T}(x) = \tanh^{-1} x$ is used.

Since equation (12) has been shown[4] to be a rigorous solution to equation (3), there remains only the need to construct the expansion coefficients A_+, A_-, $A_1(\eta)$ and $A(\eta)$

such that the solution will satisfy the appropriate boundary conditions, equations (10). Before proceeding to the determination of these expansion coefficients, however, we note that the integrated black-body function (or alternatively the temperature distribution) follows immediately from equations (4), (8) and (12):

$$B(\tau) = \frac{\bar{\sigma}}{\pi} T^4(\tau) = \frac{1}{2(\sigma w_1 + w_2)} \begin{vmatrix} \sigma \\ 1 \end{vmatrix}^T \int_{-1}^{1} \mathbf{I}(\tau, \mu)\, \mathrm{d}\mu, \tag{16a}$$

or

$$B(\tau) = \frac{1}{2(\sigma w_1 + w_2)} [A_+ + \tau A_- + \int_{-1}^{1} A(\eta)\, \mathrm{e}^{-\tau/\eta}\, \mathrm{d}\eta]. \tag{16b}$$

Similarly, the radiative heat flux is given by

$$q(\tau) = 2\pi \begin{vmatrix} 1 \\ 1 \end{vmatrix}^T \int_{-1}^{1} \mathbf{I}(\tau, \mu)\mu\, \mathrm{d}\mu, \tag{17a}$$

which simplifies to the constant

$$q = -2\pi\beta A_-, \tag{17b}$$

where we have defined

$$\beta = \frac{2}{3}\left(\frac{1}{\sigma^2} c_{12} + c_{22}\right). \tag{18}$$

We use the superscripts T and tilde interchangeably to denote the transpose operation.

If we now substitute the solution given by equation (12) into equations (10), we find that the required expansion coefficients must satisfy the following system of singular integral equations:

$$\mathbf{A}_1 + \mathbf{L}_1(\mu) = A_+ \mathbf{I}_+ + \int_0^{1/\sigma} A_1(\eta)\boldsymbol{\Phi}_1(\eta, \mu)\, \mathrm{d}\eta + \int_0^1 A(\eta)\boldsymbol{\Phi}(\eta, \mu)\, \mathrm{d}\eta, \qquad \mu \in (0, 1), \tag{19a}$$

and

$$\mathbf{A}_2 + \mathbf{L}_2(\mu) = A_- \mathbf{I}_+ + \int_0^{1/\sigma} A_1(-\eta)\boldsymbol{\Phi}_1(\eta, \mu)\, \mathrm{e}^{\tau_0/\eta}\, \mathrm{d}\eta$$

$$+ \int_0^1 A(-\eta)\boldsymbol{\Phi}(\eta, \mu)\, \mathrm{e}^{\tau_0/\eta}\, \mathrm{d}\eta, \qquad \mu \in (0, 1), \tag{19b}$$

where

$$\mathbf{L}_1(\mu) = A_+[\mathbf{B}_1^s + \mathbf{B}_1^d]\mathbf{I}_+ + A_-[\mu\mathbf{E} + \mu\mathbf{B}_1^s + \tfrac{2}{3}\mathbf{B}_1^d]\boldsymbol{\Sigma}^{-1}\mathbf{I}_+$$
$$+ \int_0^{1/\sigma} \{A_1(\eta)[\mathbf{B}_1^s\boldsymbol{\Phi}_1(-\eta,\mu) + 2\mathbf{B}_1^d\mathbf{J}_1(\eta)]$$
$$+ A_1(-\eta)[-\boldsymbol{\Phi}_1(-\eta,\mu) + \mathbf{B}_1^s\boldsymbol{\Phi}_1(\eta,\mu) + 2\mathbf{B}_1^d\mathbf{J}_1(-\eta)]\}\,d\eta$$
$$+ \int_0^1 \{A(\eta)[\mathbf{B}_1^s\boldsymbol{\Phi}(-\eta,\mu) + 2\mathbf{B}_1^d\mathbf{J}(\eta)]$$
$$+ A(-\eta)[-\boldsymbol{\Phi}(-\eta,\mu) + \mathbf{B}_1^s\boldsymbol{\Phi}(\eta,\mu) + 2\mathbf{B}_1^d\mathbf{J}(-\eta)]\}\,d\eta, \qquad \mu\in(0,1), \tag{20a}$$

and

$$\mathbf{L}_2(\mu) = A_+[\mathbf{B}_2^s + \mathbf{B}_2^d - \mathbf{E}]\mathbf{I}_+ + A_-[\tau_0(\mathbf{B}_2^s + \mathbf{B}_2^d - \mathbf{E}) + \mathbf{E} - (\mu\mathbf{E} + \mu\mathbf{B}_2^s + \tfrac{2}{3}\mathbf{B}_2^d)\boldsymbol{\Sigma}^{-1}]\mathbf{I}_+$$
$$+ \int_0^{1/\sigma} \{A_1(\eta)[\mathbf{B}_2^s\boldsymbol{\Phi}_1(\eta,\mu) - \boldsymbol{\Phi}_1(-\eta,\mu) + 2\mathbf{B}_2^d\mathbf{J}_1(-\eta)]\,e^{-\tau_0/\eta}$$
$$+ A_1(-\eta)[\mathbf{B}_2^s\boldsymbol{\Phi}_1(-\eta,\mu) + 2\mathbf{B}_2^d\mathbf{J}_1(\eta)]\,e^{\tau_0/\eta}\}\,d\eta$$
$$+ \int_0^1 \{A(\eta)[\mathbf{B}_2^s\boldsymbol{\Phi}(\eta,\mu) - \boldsymbol{\Phi}(-\eta,\mu) + 2\mathbf{B}_2^d\mathbf{J}(-\eta)]\,e^{-\tau_0/\eta}$$
$$+ A(-\eta)[\mathbf{B}_2^s\boldsymbol{\Phi}(-\eta,\mu) + 2\mathbf{B}_2^d\mathbf{J}(\eta)]\,e^{\tau_0/\eta}\}\,d\eta, \qquad \mu\in(0,1). \tag{20b}$$

Here we have used $\mathbf{E}$ to denote the unit matrix and invoked the definitions

$$\mathbf{J}_1(\eta) = \int_0^1 \boldsymbol{\Phi}_1(\eta,-\mu)\mu\,d\mu \text{ and } \mathbf{J}(\eta) = \int_0^1 \boldsymbol{\Phi}(\eta,-\mu)\mu\,d\mu. \tag{21a, b}$$

From the half-range-expansion theorem proved by SIEWERT and ZWEIFEL,[4] we know that the right-hand sides of equations (19) are sufficiently general for expansions of arbitrary two-vectors whose elements satisfy a required Hölder condition.[9] In fact, the orthogonality theorem reviewed in the H-function notation by BOND and SIEWERT[3] may be employed to solve equation (19a) in the manner

$$A_+ = \frac{1}{N_+}[\mathbf{I}_+, \mathbf{A}_1 + \mathbf{L}_1(\mu)], \tag{22a}$$

$$A_1(\eta') = \frac{1}{\eta' H(\eta') N_1(\eta')}[\boldsymbol{\Phi}_1(\eta',\mu), \mathbf{A}_1 + \mathbf{L}_1(\mu)], \qquad \eta'\in(0,1/\sigma), \tag{22b}$$

and

$$A(\eta') = \frac{1}{\eta' H(\eta') N(\eta')}[\boldsymbol{\Phi}(\eta',\mu), \mathbf{A}_1 + \mathbf{L}_1(\mu)], \qquad \eta'\in(0,1). \tag{22c}$$

Similarly, from equation (19b), we find

$$A_- = \frac{1}{N_+}[\mathbf{I}_+, \mathbf{A}_2 + \mathbf{L}_2(\mu)], \tag{23a}$$

$$A_1(-\eta') = \frac{e^{-\tau_0/\eta'}}{\eta' H(\eta') N_1(\eta')}[\mathbf{\Phi}_1(\eta', \mu), \mathbf{A}_2 + \mathbf{L}_2(\mu)], \qquad \eta' \in (0, 1/\sigma), \tag{23b}$$

and

$$A(-\eta') = \frac{e^{-\tau_0/\eta'}}{\eta' H(\eta') N(\eta')}[\mathbf{\Phi}(\eta', \mu), \mathbf{A}_2 + \mathbf{L}_2(\mu)], \qquad \eta' \in (0, 1). \tag{23c}$$

Here we have defined the scalar product by

$$[\mathbf{X}(\mu), \mathbf{Y}(\mu)] = \int_0^1 \tilde{\mathbf{X}}^\dagger(\mu)\mathbf{H}(\mu)\mathbf{Y}(\mu)\, d\mu, \tag{24}$$

with $\tilde{\mathbf{X}}^\dagger(\mu)$ denoting the transpose adjoint of the eigenvector $\mathbf{X}(\mu)$. The 'weight' matrix is given by

$$\mathbf{H}(\mu) = \begin{vmatrix} \mu H(\mu/\sigma) & 0 \\ 0 & \mu H(\mu) \end{vmatrix}, \tag{25}$$

where $H(\mu)$ is Chandrasekhar's H-function[8] for the characteristic function $\Psi(\mu) = c_{22} + c_{11}\Theta(\mu)$. Though an analytical form of $H(\mu)$ is available,[4, 10] an iterative solution of the non-linear integral equation

$$\frac{1}{H(\mu)} = \int_0^1 \nu H(\nu)\Psi(\nu)\frac{d\nu}{\nu + \mu}, \qquad \mu \in (0, 1), \tag{26}$$

provides the most efficient method for establishing $H(\mu)$ numerically. The adjoint eigenvectors and the normalization factors appearing in equations (22) and (23) follow from previously reported work:[3, 4]

$$\mathbf{I}_+^\dagger = c_{22}\begin{vmatrix} 1 \\ 1 \end{vmatrix}, \tag{27a}$$

$$\mathbf{\Phi}_1^\dagger(\eta, \mu) = M_{11}(\eta)\mathbf{G}_1(\eta, \mu) + M_{12}(\eta)\mathbf{G}_2(\eta, \mu), \tag{27b}$$

and

$$\mathbf{\Phi}^\dagger(\eta, \mu) = [M_{21}(\eta)\mathbf{G}_1(\eta, \mu) + M_{22}(\eta)\mathbf{G}_2(\eta, \mu)]\Theta(\eta) + \mathbf{\Phi}_3^\dagger(\eta, \mu)[1 - \Theta(\eta)] \tag{27c}$$

where $\mathbf{G}_1(\eta, \mu)$, $\mathbf{G}_2(\eta, \mu)$, and $\mathbf{\Phi}_3^\dagger(\eta, \mu)$ follow respectively from equations (13c), (14a), and (14b) by replacing c_{ij} with c_{ji}. The functions $M_{ij}(\eta)$ are listed in Appendix A. In addition, the normalization factors are

$$N_+ = c_{22}\sqrt{\beta}, \tag{28a}$$

$$N_1(\eta) = [1 - 2\eta c_{11}\mathcal{F}(\sigma\eta) - 2\eta c_{22}\mathcal{F}(\eta)]^2 + \pi^2\eta^2(c_{11} + c_{22})^2, \tag{28b}$$

and

$$N(\eta) = \left[1 - 2\eta c_{22}\mathscr{T}(\eta) - 2\eta c_{11}\left\{\Theta(\eta)\mathscr{T}(\sigma\eta) + [1 - \Theta(\eta)]\mathscr{T}\left(\frac{1}{\sigma\eta}\right)\right\}\right]^2 + \pi^2\eta^2\Psi^2(\eta). \quad (28c)$$

It is quite clear (by comparison, for example, with the analysis reported by ÖZIŞIK and SIEWERT[11] for the grey analogue to this problem) that since $\mathbf{L}_1(\mu)$ and $\mathbf{L}_2(\mu)$ are themselves expressed in terms of expansion coefficients, equations (22) and (23) yield coupled integral equations, rather than the closed-form results obtained for typical half-space problems.[3]

If we now write the sought expansion coefficients in the forms

$$\mathbf{A} = \begin{vmatrix} A_+ \\ A_- \end{vmatrix}, \qquad \mathbf{A}_1(\eta) = \begin{vmatrix} A_1(\eta) \\ A_1(-\eta) \end{vmatrix}, \quad \text{and } \mathbf{A}(\eta) = \begin{vmatrix} A(\eta) \\ A(-\eta) \end{vmatrix}, \quad (29a, b, c)$$

equations (22) and (23) can be written more explicitly in matrix notation:

$$\mathbf{SA} = \mathbf{G} + \int_0^{1/\sigma} \mathbf{U}(\eta)\mathbf{A}_1(\eta)\,d\eta + \int_0^1 \mathbf{V}(\eta)\mathbf{A}(\eta)\,d\eta, \quad (30a)$$

$$\mathbf{S}_1(\eta')\mathbf{A}_1(\eta') = \mathbf{G}_1(\eta') + \mathbf{W}_1(\eta')\mathbf{A} + \int_0^{1/\sigma} \mathbf{U}_1(\eta, \eta')\mathbf{A}_1(\eta)\,d\eta + \int_0^1 \mathbf{V}_1(\eta, \eta')\mathbf{A}(\eta)\,d\eta, \qquad \eta' \in (0, 1/\sigma), \quad (30b)$$

and

$$\mathbf{S}(\eta')\mathbf{A}(\eta') = \mathbf{G}(\eta') + \mathbf{W}(\eta')\mathbf{A} + \int_0^{1/\sigma} \mathbf{U}(\eta, \eta')\mathbf{A}_1(\eta)\,d\eta + \int_0^1 \mathbf{V}(\eta, \eta')\mathbf{A}(\eta)\,d\eta, \qquad \eta' \in (0, 1), \quad (30c)$$

where, for the sake of continuity, we defer the definitions of all new, but known, functions to Appendix B. The 'cross-product' integrals required here are listed in Appendix A for reference. Further, in writing equations (30), we have made the assumption that the specular reflection at the boundary surfaces is grey, i.e. we have taken

$$\mathbf{B}_\alpha^s = \rho_\alpha^s\mathbf{E}, \qquad \alpha = 1 \text{ or } 2. \quad (31)$$

We note that the assumption here of grey specular reflection can be relaxed; however, the ensuing complications are considerable. For non-grey specular reflection, equations (30) remain singular, as opposed to the regular nature of those equations for grey specular reflection. Though a procedure similar to that used by KUSZELL[12] for a two-media problem related to the grey equation of transfer can be followed to regularize equations (30) for the case of non-grey specular reflection, we do not report the required analysis here. Since non-grey diffuse reflection is considered in the present work and since there appears

to be little difference between the effects of specular and diffuse reflection, we do not consider non-grey specular reflection.

It is rather unlikely that analytical solutions to equations (30) exist, and thus two procedures may be pursued: either reasonably tractable approximate solutions may be obtained analytically for $\mathbf{A}$, $\mathbf{A}_1(\eta)$, $\mathbf{A}(\eta)$, or, as discussed in the next section, accurate numerical solutions may be computed by solving these regular integral equations iteratively. We obtain our lowest-order approximate solution by neglecting entirely the continuum coefficients in equations (30):

$$\mathbf{A}_1^{(1)}(\eta) = \mathbf{O}, \qquad \mathbf{A}^{(1)}(\eta) = \mathbf{O}, \quad \text{and} \quad \mathbf{A}^{(1)} = \mathbf{S}^{-1}\mathbf{G}. \tag{32a, b, c}$$

Similarly, the next-order approximation is developed by substituting equations (32) into the right-hand sides of equations (30b) and (30c) to find

$$\mathbf{A}_1^{(2)}(\eta') = \mathbf{S}_1^{-1}(\eta')[\mathbf{G}_1(\eta') + \mathbf{W}_1(\eta')\mathbf{S}^{-1}\mathbf{G}], \qquad \eta' \in (0, 1/\sigma), \tag{33a}$$

and

$$\mathbf{A}^{(2)}(\eta') = \mathbf{S}^{-1}(\eta')[\mathbf{G}(\eta') + \mathbf{W}(\eta')\mathbf{S}^{-1}\mathbf{G}], \qquad \eta' \in (0, 1); \tag{33b}$$

these results can now be entered into equation (30a) to yield

$$\mathbf{A}^{(2)} = \mathbf{S}^{-1}\Big\{\mathbf{G} + \int_0^{1/\sigma} \mathbf{U}(\eta)\mathbf{S}_1^{-1}(\eta)[\mathbf{G}_1(\eta) + \mathbf{W}_1(\eta)\mathbf{S}^{-1}\mathbf{G}]\,d\eta + \int_0^1 \mathbf{V}(\eta)\mathbf{S}^{-1}(\eta)[\mathbf{G}(\eta) + \mathbf{W}(\eta)\mathbf{S}^{-1}\mathbf{G}]\,d\eta\Big\}. \tag{33c}$$

In the next section the accuracy of these two analytical approximations is investigated by comparing each to our 'exact' numerical solutions of equations (30).

Equations (30) are the basic equations to be solved for the general case of non-grey emitting and diffusely reflecting, and grey specularly reflecting boundaries, and, as such, contain many special cases. In particular, for the special case without specular reflection, we find it convenient (for purposes of reporting our computations) to write the desired solution in terms of an albedo problem independent of surface parameters. If we let $\mathbf{\Psi}(\tau, \mu)$ denote a 2×2 *matrix* solution of equation (3) such that

$$\mathbf{\Psi}(0, \mu) = \mathbf{E}, \qquad \mu \in (0, 1), \tag{34a}$$

and

$$\mathbf{\Psi}(\tau_0, -\mu) = \mathbf{O}, \qquad \mu \in (0, 1), \tag{34b}$$

then the solution $\mathbf{I}(\tau, \mu)$ to equation (3) which satisfies

$$\mathbf{I}(0, \mu) = \mathbf{A}_1 + 2\mathbf{B}_1^d \int_0^1 \mathbf{I}(0, -\mu')\mu'\,d\mu', \qquad \mu \in (0, 1), \tag{35a}$$

and

$$\mathbf{I}(\tau_0, -\mu) = \mathbf{A}_2 + 2\mathbf{B}_1^d \int_0^1 \mathbf{I}(\tau_0, \mu')\mu'\,d\mu', \qquad \mu \in (0, 1), \tag{35b}$$

can be expressed as

$$\mathbf{I}(\tau, \mu) = \mathbf{\Psi}(\tau, \mu)\mathbf{L} + \mathbf{\Psi}(\tau_0 - \tau, -\mu)\mathbf{R}. \tag{36}$$

Here the two vectors **L** and **R** are the easily established solutions of the algebraic equations

$$\mathbf{L} = \mathbf{A}_1 + 2\mathbf{B}_1^d[\mathbf{PL} + \mathbf{QR}] \tag{37a}$$

and

$$\mathbf{R} = \mathbf{A}_2 + 2\mathbf{B}_2^d[\mathbf{QL} + \mathbf{PR}], \tag{37b}$$

where **P** and **Q** can be computed from the solution of the albedo problem:

$$\mathbf{P} = \int_0^1 \mathbf{\Psi}(0, -\mu)\mu \, d\mu \tag{38a}$$

and

$$\mathbf{Q} = \int_0^1 \mathbf{\Psi}(\tau_0, \mu)\mu \, d\mu. \tag{38b}$$

We note that since

$$\begin{vmatrix} 1 \\ 1 \end{vmatrix}^T [\mathbf{P} + \mathbf{Q}] = \frac{1}{2} \begin{vmatrix} 1 \\ 1 \end{vmatrix}^T, \tag{39}$$

a maximum of six of the eight matrix elements defined by equations (38) are independent.

In terms of this basic albedo problem, we write the heat flux and the temperature distribution as

$$q = 2\pi \begin{vmatrix} 1 \\ 1 \end{vmatrix}^T \mathbf{Q}[\mathbf{L} - \mathbf{R}] \tag{40}$$

and

$$\frac{\bar{\sigma}}{\pi} T^4(\tau) = \mathbf{\Gamma}(\tau)\mathbf{L} + \mathbf{\Gamma}(\tau_0 - \tau)\mathbf{R}, \tag{41}$$

where we have invoked the definition

$$\mathbf{\Gamma}(\tau) = \frac{1}{2(\sigma w_1 + w_2)} \begin{vmatrix} \sigma \\ 1 \end{vmatrix}^T \int_{-1}^1 \mathbf{\Psi}(\tau, \mu) \, d\mu. \tag{42}$$

3. NUMERICAL ANALYSIS AND RESULTS

As noted previously, equation (12) is a rigorous solution of the considered equation of transfer; however, upon constraining that general solution to meet the boundary conditions represented by equations (10), we obtained equations (30), the coupled integral equations from which the required expansion coefficients must be determined. Thus, in contrast to typical half-space applications[4] for which solutions for the expansion

coefficients can be written in closed form, we must solve equations (30) iteratively to yield the final 'exact' semi-analytical result. On the other hand, equations (12), (32) and (33) are tractable analytical approximate solutions. Clearly, once the expansion coefficients are determined, the radiative flux and the temperature distribution (and any other moment of the radiation intensity) will follow immediately from equations (12), (16) and (17).

Using an improved Gaussian-quadrature scheme[13] to evaluate the integral terms, we have solved equations (30) iteratively to yield numerical results for all expansion coefficients. The analytical approximations given by equations (32) were used to initiate the calculation, and the iterative procedure was terminated when successive iterates yielded expansion coefficients in agreement to at least ten significant figures. For all cases studied, convergence was achieved in an average of 8 and a maximum of 24 iterations. It was observed, as expected, that convergence became less rapid as the slab thickness was decreased.

All computations were performed in double-precision arithmetic on an IBM 360/75 computer, and the 81-point improved Gaussian-quadrature scheme[13] was the basic method used to evaluate required integrals. For most cases studied, an 81-point scheme in each of the intervals $(0, 1/\sigma)$ and $(1/\sigma, 1)$ provided results of sufficient accuracy; however, in a few cases (specifically for large σ and small w_1) it was necessary to subdivide the interval $(1/\sigma, 1)$ and to apply the 81-point scheme in each subinterval. The H-functions required in the calculations were constructed by solving equation (26) iteratively in the usual manner.[3]

In contrast to SIMMONS and FERZIGER's work,[7] where only black boundaries were considered, we encounter here the need to evaluate numerically Cauchy principal-value integrals, which arise as a consequence of various scalar products and are characterized by equations (A-16) of Appendix A. These integrals can be evaluated from the expression[14]

$$P\int_0^a \mu H(\mu)\frac{d\mu}{\mu-\eta} = \int_0^a [\mu H(\mu) - \eta H(\eta)]\frac{d\mu}{\mu-\eta} + \eta H(\eta)\ln\left(\frac{a-\eta}{\eta}\right), \qquad \eta\in(0,a), \quad (43)$$

which, of course, requires the derivative of $H(\mu)$. Rather than compute this derivative from the H-function tabulations, a procedure surely to be avoided, we prefer to base this calculation on

$$\mu\frac{d}{d\mu}H(\mu) = \mu H^2(\mu)\int_0^1 \eta\Psi(\eta)H(\eta)\frac{d\eta}{(\eta+\mu)^2}, \qquad \mu\in(0,1), \quad (44)$$

a form resulting from the non-linear H-equation.

Since we consider the calculations reported here to be highly accurate, we would like to mention several checks employed to substantiate confidence in our results. To develop one such check, the calculations were performed with an integration scheme having N nodal points and then repeated with a scheme having $2N$ nodal points. This doubling procedure was continued until two successive calculations failed to alter the reported values. For the albedo problem, a check of computed values of the matrices $\mathbf{Q}$ and $\mathbf{P}$ is provided by equation (39), which was verified to at least five significant figures for all cases considered. The basic test of the computed expansion coefficients is how accurately the boundary conditions, equations (10), are satisfied. Since the distributional nature of the continuum

eigenvectors limits the accuracy of a pointwise verification of the boundary conditions, we have chosen to consider, instead, various moments of equations (10). To illustrate these checks, we consider equations (10) rearranged and written symbolically as $\mathbf{L}(\mu) = \mathbf{R}(\mu)$, $\mu \in (0, 1)$. We have computed

$$\int_0^1 \mathbf{L}(\mu)\mu^k \, d\mu \quad \text{and} \quad \int_0^1 \mathbf{R}(\mu)\mu^k \, d\mu, \qquad k = 0, 1, 2, \ldots, 10,$$

and found agreement consistent with the data reported herein. Although the above checks do not rigorously guarantee the accuracy of our results, we believe that the number and diversity of these checks provide a reasonable degree of confidence in our reported values.

We should now like to present the results of numerical solutions to the albedo problem for a wide variety of cases. In Tables 1–3, we list a choice of six elements of the matrices **P** and **Q** for representative values of the parameters σ, w_1 and τ_0. These values plus equation (39) permit the calculation of the radiative heat flux for diffusely reflecting problems through equation (40), with **L** and **R** being evaluated from equations (37). Table 4 is devoted to a compilation of the elements $\Gamma_1(\tau)$ and $\Gamma_2(\tau)$ of $\mathbf{\Gamma}(\tau)$ required in equation (41) to evaluate the temperature distribution, again for diffusely reflecting problems. Thus,

TABLE 1. SIX ELEMENTS OF **P** AND **Q** REQUIRED FOR DIFFUSE PROBLEMS WITH $\sigma = 2$

w_1	τ_0	P_{11}	P_{12}	P_{21}	Q_{12}	Q_{21}	Q_{22}
0.1	0.1	0.012404	0.0069553	0.062597	0.0067931	0.061138	0.45103
0.1	0.5	0.030880	0.020657	0.18591	0.016842	0.15158	0.33472
0.1	1.0	0.038264	0.028140	0.25326	0.017796	0.16017	0.25775
0.1	2.0	0.043789	0.034939	0.31445	0.014180	0.12762	0.17911
0.1	10.0	0.051346	0.045214	0.40693	0.0042888	0.038599	0.052970
0.3	0.1	0.032546	0.018254	0.042592	0.017838	0.041622	0.43994
0.3	0.5	0.085250	0.057245	0.13357	0.047123	0.10995	0.30357
0.3	1.0	0.10816	0.080254	0.18726	0.051933	0.12118	0.22159
0.3	2.0	0.12567	0.10178	0.23749	0.042802	0.099872	0.14729
0.3	10.0	0.14873	0.13371	0.31198	0.012895	0.030087	0.042172
0.5	0.1	0.048202	0.027039	0.027039	0.026434	0.026434	0.43131
0.5	0.5	0.13172	0.088715	0.088715	0.073589	0.073589	0.27642
0.5	1.0	0.17091	0.12778	0.12778	0.084339	0.084339	0.18749
0.5	2.0	0.20184	0.16574	0.16574	0.072137	0.072137	0.11504
0.5	10.0	0.24152	0.22154	0.22154	0.021748	0.021748	0.031126
0.7	0.1	0.060721	0.034066	0.014600	0.033314	0.014277	0.42440
0.7	0.5	0.17197	0.11612	0.049765	0.096925	0.041539	0.25252
0.7	1.0	0.22795	0.17156	0.073524	0.11520	0.049369	0.15518
0.7	2.0	0.27395	0.22783	0.097642	0.10253	0.043942	0.081973
0.7	10.0	0.33213	0.31088	0.13323	0.031128	0.013341	0.019501
0.9	0.1	0.070960	0.039814	0.0044238	0.038946	0.0043273	0.41875
0.9	0.5	0.20724	0.14022	0.015580	0.11765	0.013073	0.23133
0.9	1.0	0.28031	0.21217	0.023575	0.14464	0.016071	0.12449
0.9	2.0	0.34318	0.28884	0.032094	0.13427	0.014919	0.047760
0.9	10.0	0.42279	0.40405	0.044895	0.041402	0.0046002	0.0068754

TABLE 2. SIX ELEMENTS OF P AND Q REQUIRED FOR DIFFUSE PROBLEMS WITH $\sigma = 5$

w_1	τ_0	P_{11}	P_{12}	P_{21}	Q_{12}	Q_{21}	Q_{22}
0.1	0.1	0.040449	0.011537	0.10384	0.011037	0.099335	0.44666
0.1	0.5	0.063160	0.026121	0.23509	0.018303	0.16472	0.33193
0.1	1.0	0.066952	0.031570	0.28413	0.015337	0.13803	0.25827
0.1	2.0	0.069678	0.036407	0.32766	0.010753	0.096774	0.18072
0.1	10.0	0.073753	0.043997	0.39598	0.0031748	0.028573	0.053442
0.3	0.1	0.087508	0.025083	0.058527	0.024083	0.056194	0.43346
0.3	0.5	0.15433	0.067162	0.15671	0.049208	0.11482	0.29862
0.3	1.0	0.16731	0.085398	0.19926	0.044479	0.10378	0.22440
0.3	2.0	0.17537	0.10073	0.23503	0.031632	0.073808	0.15376
0.3	10.0	0.18635	0.12341	0.28795	0.0091302	0.021304	0.044264
0.5	0.1	0.11412	0.032791	0.032791	0.031541	0.031541	0.42592
0.5	0.5	0.21999	0.098966	0.098966	0.074663	0.074663	0.27166
0.5	1.0	0.24484	0.13286	0.13286	0.073415	0.073415	0.19190
0.5	2.0	0.25927	0.16141	0.16141	0.054121	0.054121	0.12586
0.5	10.0	0.27685	0.20119	0.20119	0.015272	0.015272	0.034909
0.7	0.1	0.13125	0.037768	0.016186	0.036369	0.015587	0.42105
0.7	0.5	0.27090	0.12477	0.053472	0.096098	0.041185	0.24919
0.7	1.0	0.31036	0.17715	0.075921	0.10303	0.044155	0.15946
0.7	2.0	0.33359	0.22398	0.095991	0.080860	0.034654	0.094013
0.7	10.0	0.35881	0.28627	0.12269	0.022413	0.0096056	0.024200
0.9	0.1	0.14320	0.041248	0.0045831	0.039749	0.0044165	0.41764
0.9	0.5	0.31206	0.14628	0.016254	0.11442	0.012713	0.23011
0.9	1.0	0.36876	0.21982	0.024425	0.13368	0.014854	0.12648
0.9	2.0	0.40512	0.29339	0.032599	0.11537	0.012819	0.054490
0.9	10.0	0.44154	0.39162	0.043513	0.032087	0.0035653	0.010050

both the heat flux and temperature distribution for a problem with any type of diffuse boundaries (as characterized by equations (35)) are easily obtained from the information in Tables 1–4.

We have investigated the effects of purely specular as opposed to purely diffuse reflection on both the net radiative heat flux and the temperature distribution within the medium. Figure 1 shows the temperature distribution for each type of reflection, with the surfaces at $\tau = 0$ and $\tau = \tau_0$ maintained at temperatures T_1 and zero respectively. To emphasize the effects of reflectivity, we have taken the wall at $\tau = 0$ to be opaque and highly reflective by choosing $\varepsilon_{11} = \varepsilon_{12} = 0.1$, and the surface at $\tau = \tau_0$ to be non-reflecting. The temperature distribution within the medium is slightly higher with specular reflection than with diffuse reflection. The magnitude of the corresponding heat flux, however, is smaller with specularly reflecting walls than with diffusely reflecting walls; but the difference is less than one percent, and we do not present these results. Analogous comparisons for various other values of σ, w_1, τ_0 have led to similar conclusions. To characterize the difference in temperature between specularly and diffusely reflecting cases, we present in Table 5 the percent differences in the resulting temperature distributions for selected cases.

To illustrate the effects of non-grey boundaries on the temperature distribution, we consider a slab with a diffusely reflecting and emitting boundary at $\tau = 0$ maintained at temperature T_1, and a non-reflecting boundary at $\tau = \tau_0$ maintained at zero temperature.

TABLE 3. SIX ELEMENTS OF **P** AND **Q** REQUIRED FOR DIFFUSE PROBLEMS WITH $\sigma = 10$

w_1	τ_0	P_{11}	P_{12}	P_{21}	Q_{12}	Q_{21}	Q_{22}
0.1	0.1	0.079747	0.014709	0.13238	0.013756	0.12380	0.44375
0.1	0.5	0.096882	0.026891	0.24202	0.016556	0.14900	0.33268
0.1	1.0	0.098978	0.030990	0.27891	0.012882	0.11594	0.25985
0.1	2.0	0.10079	0.034953	0.31458	0.0089564	0.080607	0.18200
0.1	10.0	0.10360	0.041268	0.37141	0.0026469	0.023822	0.053876
0.3	0.1	0.15164	0.028617	0.066774	0.027008	0.063019	0.43026
0.3	0.5	0.20834	0.066668	0.15556	0.044294	0.10335	0.30161
0.3	1.0	0.21465	0.079910	0.18646	0.035970	0.083930	0.23104
0.3	2.0	0.21912	0.091551	0.21362	0.024871	0.058033	0.15960
0.3	10.0	0.22559	0.10928	0.25499	0.0071990	0.016798	0.046209
0.5	0.1	0.18553	0.035335	0.035335	0.033469	0.033469	0.42371
0.5	0.5	0.27989	0.098019	0.098019	0.068532	0.068532	0.27540
0.5	1.0	0.29233	0.12395	0.12395	0.060221	0.060221	0.20238
0.5	2.0	0.29949	0.14514	0.14514	0.041995	0.041995	0.13656
0.5	10.0	0.30893	0.17554	0.17554	0.011866	0.011866	0.038439
0.7	0.1	0.20534	0.039298	0.016842	0.037295	0.015983	0.41983
0.7	0.5	0.33365	0.12465	0.053422	0.090400	0.038743	0.25221
0.7	1.0	0.35552	0.16885	0.072363	0.088528	0.037941	0.17035
0.7	2.0	0.36671	0.20499	0.087852	0.064367	0.027586	0.10805
0.7	10.0	0.37940	0.25298	0.10842	0.017653	0.0075657	0.028957
0.9	0.1	0.21834	0.041914	0.0046571	0.039825	0.0044250	0.41727
0.9	0.5	0.37713	0.14802	0.016446	0.11034	0.012260	0.23132
0.9	1.0	0.41316	0.21827	0.024252	0.12349	0.013721	0.13215
0.9	2.0	0.43249	0.28360	0.031511	0.10062	0.011180	0.064788
0.9	10.0	0.45061	0.36610	0.040678	0.026969	0.0029966	0.014146

Figure 2 shows the temperature distribution for grey and non-grey wall conditions. The upper and lower curves are for opaque non-grey walls with $\varepsilon_{11} = 0.9$, $\varepsilon_{12} = 0.1$ and $\varepsilon_{11} = 0.1$, $\varepsilon_{12} = 0.9$ respectively, whereas the middle curve is for opaque grey walls with $\varepsilon_{11} = \varepsilon_{12} = 0.5$. Clearly, there is a significant difference in the temperature distributions for grey as opposed to non-grey walls. Figure 3 displays results similar to those of Fig. 2, but with $\sigma = 10$; we note that there is an increase in the difference in the temperatures for the grey and non-grey cases for the larger value of σ.

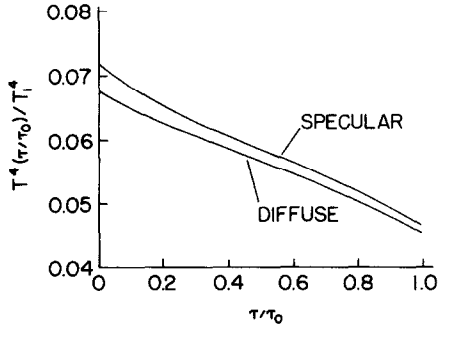

FIG. 1. Temperature distributions resulting from specular and diffuse reflection for opaque walls and $w_1 = 0.5$, $\tau_0 = 0.1$, $\sigma = 2$ and $\varepsilon_{11} = \varepsilon_{12} = 0.1$.

TABLE 4. THE TEMPERATURE FUNCTION $\Gamma(\tau/\tau_0)$

			τ/τ_0										
			0.0	0.1	0.2	0.3	0.4	0.5	0.6	0.7	0.8	0.9	1.0
σ	w_1	τ_0	$\Gamma_1(\tau/\tau_0)$										
2.0	0.3	0.1	0.8992	0.8498	0.8116	0.7772	0.7450	0.7142	0.6844	0.6550	0.6255	0.5952	0.5605
2.0	0.3	1.0	1.1272	0.9155	0.7866	0.6846	0.5984	0.5225	0.4536	0.3895	0.3279	0.2664	0.1941
2.0	0.5	0.1	0.7925	0.7521	0.7201	0.6909	0.6632	0.6364	0.6101	0.5839	0.5574	0.5298	0.4976
2.0	0.5	1.0	1.0193	0.8597	0.7541	0.6660	0.5881	0.5170	0.4504	0.3867	0.3244	0.2609	0.1853
2.0	0.9	0.1	0.6407	0.6116	0.5877	0.5653	0.5437	0.5224	0.5012	0.4797	0.4577	0.4343	0.4064
2.0	0.9	1.0	0.8618	0.7699	0.6977	0.6308	0.5664	0.5036	0.4416	0.3796	0.3168	0.2513	0.1719
5.0	0.3	0.1	1.4365	1.2999	1.2007	1.1142	1.0354	0.9618	0.8917	0.8238	0.7567	0.6883	0.6091
5.0	0.3	1.0	1.6678	1.0987	0.8238	0.6450	0.5187	0.4239	0.3488	0.2854	0.2283	0.1723	0.1028
5.0	0.5	0.1	1.0942	1.0042	0.9357	0.8741	0.8165	0.7614	0.7077	0.6547	0.6012	0.5455	0.4792
5.0	0.5	1.0	1.3254	0.9876	0.7939	0.6515	0.5399	0.4484	0.3702	0.3007	0.2358	0.1714	0.0938
5.0	0.9	0.1	0.7424	0.6910	0.6495	0.6109	0.5735	0.5369	0.5004	0.4635	0.4256	0.3852	0.3360
5.0	0.9	1.0	0.9671	0.8423	0.7451	0.6558	0.5715	0.4905	0.4119	0.3349	0.2583	0.1805	0.0897
			τ/τ_0										
			0.0	0.1	0.2	0.3	0.4	0.5	0.6	0.7	0.8	0.9	1.0
σ	w_1	τ_0	$\Gamma_2(\tau/\tau_0)$										
2.0	0.3	0.1	0.4567	0.4469	0.4375	0.4280	0.4182	0.4082	0.3978	0.3868	0.3752	0.3624	0.3463
2.0	0.3	1.0	0.6438	0.6311	0.6038	0.5700	0.5319	0.4904	0.4458	0.3982	0.3472	0.2910	0.2185
2.0	0.5	0.1	0.4031	0.3960	0.3885	0.3806	0.3723	0.3636	0.3544	0.3446	0.3340	0.3221	0.3069
2.0	0.5	1.0	0.5885	0.5966	0.5807	0.5546	0.5215	0.4830	0.4400	0.3926	0.3408	0.2828	0.2069
2.0	0.9	0.1	0.3265	0.3225	0.3174	0.3116	0.3053	0.2984	0.2909	0.2828	0.2738	0.2636	0.2501
2.0	0.9	1.0	0.5067	0.5405	0.5405	0.5257	0.5006	0.4674	0.4272	0.3809	0.3285	0.2686	0.1894
5.0	0.3	0.1	0.3102	0.3153	0.3151	0.3125	0.3081	0.3021	0.2946	0.2855	0.2746	0.2612	0.2417
5.0	0.3	1.0	0.4919	0.5976	0.6158	0.6035	0.5737	0.5326	0.4831	0.4264	0.3619	0.2863	0.1779
5.0	0.5	0.1	0.2388	0.2454	0.2468	0.2458	0.2430	0.2386	0.2328	0.2254	0.2163	0.2049	0.1878
5.0	0.5	1.0	0.4183	0.5583	0.6019	0.6072	0.5881	0.5516	0.5018	0.4407	0.3684	0.2826	0.1625
5.0	0.9	0.1	0.1638	0.1702	0.1722	0.1722	0.1707	0.1679	0.1639	0.1586	0.1518	0.1432	0.1301
5.0	0.9	1.0	0.3400	0.5099	0.5847	0.6151	0.6132	0.5853	0.5362	0.4687	0.3850	0.2846	0.1496

TABLE 5. TEMPERATURE COMPARISONS BETWEEN SPECULAR AND DIFFUSE REFLECTION FOR THE CASE OF OPAQUE WALLS AND $w_1 = 0.5$, $\sigma = 2$ AND $\varepsilon_{11} = \varepsilon_{12}$

		τ/τ_0		
		0.0	0.5	1.0
		$\frac{T_s^4(\tau/\tau_0) - T_d^4(\tau/\tau_0)}{T_d^4(\tau/\tau_0)} \times 100$		
τ_0	ε_{11}			
0.1	0.9	0.6	0.3	0.2
0.1	0.5	3.2	1.6	1.1
0.1	0.1	5.9	3.1	2.1
1.0	0.9	0.4	0.1	0.1
1.0	0.5	2.4	0.2	0.2
1.0	0.1	5.0	1.0	0.3

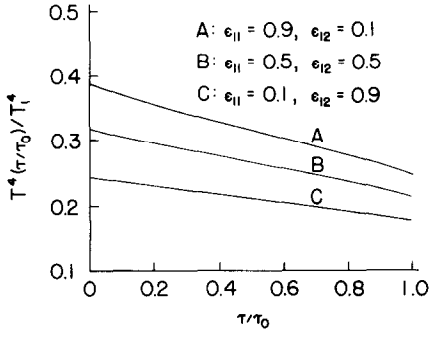

FIG. 2. Temperature distributions resulting from diffuse reflection and various opaque wall conditions for $w_1 = 0.5$, $\tau_0 = 0.1$ and $\sigma = 2$.

Though we have, in fact, solved equations (30) to obtain the 'exact' results quoted here, we should like to emphasize that the second-order analytical approximation given by equations (33) is sufficiently accurate for many engineering applications. To illustrate the accuracy of the two analytical approximations, and to provide accurate numerical results for several examples of the most general problem discussed here, we list in Table 7 the heat flux and the temperature distribution for the six cases defined in Table 6. We note that Table 6 includes cases with both opaque and partially transparent wall conditions.

TABLE 6. DATA FOR SIX SELECTED CASES

Case	σ	w_1	τ_0	ε_{11}	ε_{12}	ε_{21}	ε_{22}	ρ_{11}^d	ρ_{12}^d	ρ_{21}^d	ρ_{22}^d	ρ_1^s	ρ_2^s	T_1/T_2
I	2.0	0.6	0.5	0.2	0.4	0.3	0.2	0.7	0.5	0.5	0.6	0.1	0.2	2.0
II	2.0	0.4	0.5	0.5	0.2	0.1	0.3	0.1	0.4	0.4	0.2	0.4	0.3	2.0
III	2.0	0.4	1.0	0.5	0.2	0.1	0.3	0.1	0.4	0.4	0.2	0.4	0.3	2.0
IV	2.0	0.5	1.5	0.1	0.3	0.6	0.1	0.6	0.5	0.2	0.7	0.2	0.1	2.0
V	5.0	0.6	1.0	0.8	0.6	0.5	0.3	0.1	0.3	0.2	0.1	0.1	0.2	2.0
VI	5.0	0.5	1.5	0.1	0.3	0.6	0.1	0.6	0.5	0.2	0.7	0.2	0.1	2.0

TABLE 7. THE TEMPERATURE DISTRIBUTION AND HEAT FLUX FOR SELECTED CASES

Case*		τ/τ_0 = 0.0	0.1	0.2	0.3	0.4	0.5	0.6	0.7	0.8	0.9	1.0	$q/\sigma T_1^4$
		$T^4(\tau/\tau_0)/T_1^4$											
I	(a)	0.614	0.608	0.601	0.595	0.588	0.581	0.575	0.568	0.561	0.555	0.548	0.1237
	(b)	0.596	0.585	0.575	0.565	0.556	0.547	0.537	0.527	0.516	0.505	0.489	0.1327
	(c)	0.59365	0.58223	0.57267	0.56345	0.55427	0.54498	0.53544	0.52550	0.51491	0.50316	0.48746	0.13182
II	(a)	0.446	0.438	0.430	0.422	0.414	0.406	0.398	0.390	0.383	0.375	0.367	0.1697
	(b)	0.539	0.514	0.496	0.480	0.466	0.452	0.438	0.424	0.411	0.396	0.379	0.1811
	(c)	0.53888	0.51387	0.49607	0.48045	0.46605	0.45240	0.43922	0.42626	0.41323	0.39961	0.38280	0.18522
III	(a)	0.488	0.474	0.459	0.444	0.429	0.415	0.400	0.385	0.371	0.356	0.341	0.1568
	(b)	0.583	0.545	0.517	0.493	0.471	0.450	0.430	0.409	0.389	0.368	0.342	0.1708
	(c)	0.57940	0.54050	0.51346	0.48977	0.46787	0.44704	0.42684	0.40691	0.38683	0.36581	0.33946	0.16995
IV	(a)	0.448	0.432	0.416	0.401	0.385	0.369	0.353	0.337	0.321	0.305	0.289	0.1061
	(b)	0.413	0.397	0.381	0.365	0.348	0.331	0.312	0.292	0.271	0.246	0.211	0.1081
	(c)	0.42105	0.40445	0.38876	0.37262	0.35589	0.33849	0.32028	0.30098	0.28009	0.25641	0.22315	0.10804
V	(a)	0.677	0.644	0.612	0.580	0.547	0.515	0.483	0.450	0.418	0.386	0.354	0.2240
	(b)	0.877	0.786	0.719	0.659	0.604	0.552	0.502	0.453	0.403	0.350	0.284	0.2430
	(c)	0.83545	0.74940	0.68657	0.63048	0.57804	0.52759	0.47792	0.42792	0.37623	0.32048	0.24742	0.24233
VI	(a)	0.509	0.492	0.475	0.459	0.442	0.425	0.408	0.392	0.375	0.358	0.341	0.0896
	(b)	0.384	0.379	0.368	0.353	0.334	0.313	0.287	0.257	0.219	0.170	0.088	0.0968
	(c)	0.46176	0.44769	0.43114	0.41284	0.39312	0.37192	0.34882	0.32290	0.29244	0.25381	0.19009	0.09648

* (a) First approximation. (b) Second approximation. (c) 'Exact' result.

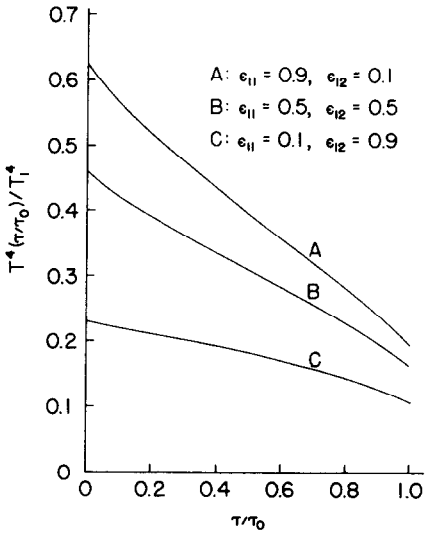

FIG. 3. Temperature distributions resulting from diffuse reflection and various opaque wall conditions for $w_1 = 0.5$, $\tau_0 = 0.1$ and $\sigma = 10$.

The entries in Table 7 represent the prediction of the first- and second-order approximations and the 'exact' values.

In conclusion, we note that, as for the grey model,[11] the analysis here may be easily modified to include particular solutions required for similar problems with inhomogeneous source terms. In addition, since the normal modes and relevant expansion and orthogonality theorems have been reported,[15] the present work may be generalized to the 3-, 4-, $\cdots$ N-band model.

Acknowledgement—This work was supported in part by the National Science Foundation through grant GK 11935.

REFERENCES

1. S. CHANDRASEKHAR, *Mon. Not. R. Astr. Soc.* **96,** 21 (1935).
2. G. MÜNCH, *Astrophys. J.* **104,** 87 (1946).
3. G. R. BOND and C. E. SIEWERT, *JQSRT* **10,** 865 (1970).
4. C. E. SIEWERT and P. F. ZWEIFEL, *Ann. Phys.* **36,** 61 (1966).
5. W. LICK, Energy transfer by radiation and conduction, *Proc. of the* 1963 *Heat Transfer and Fluid Mechanics Institute*, pp. 14–26. Stanford University Press, Stanford (1963).
6. R. GREIF, *Int. J. Heat Mass Trans.* **7,** 891 (1964).
7. G. M. SIMMONS and J. H. FERZIGER, *Int. J. Heat Mass Transfer* **11,** 1611 (1968).
8. S. CHANDRASEKHAR, *Radiative Transfer*. Oxford University Press, London (1950).
9. N. I. MUSKHELISHVILI, *Singular Integral Equations*. Noordhoff, Groningen, Holland (1953).
10. C. E. SIEWERT and M. N. ÖZIŞIK, *Mon. Not. R. Astr. Soc.* **146,** 351 (1969).
11. M. N. ÖZIŞIK and C. E. SIEWERT, *Int. J. Heat Mass Transfer* **12,** 611 (1969).
12. A. KUSZELL, *Acta Phys. Pol.* **20,** 567 (1961).
13. A. S. KRONROD, *Nodes and Weights of Quadrature Formulas*. Consultants Bureau, New York (1965).
14. K. M. CASE and P. F. ZWEIFEL, *Linear Transport Theory*. Addison-Wesley, Reading, Mass. (1967).
15. C. E. SIEWERT and P. F. ZWEIFEL, *J. Math. Phys.* **7,** 2092 (1966).

As discussed in the main text of this paper, equations (30) were developed by 'taking' scalar products of the boundary conditions written in the form of equations (19), and by then invoking the appropriate half-range orthogonality theorem.[3,4] In so doing, we encounter the need to evaluate many 'cross-product' integrals, and though most of the pertinent relations are available,[7] we should like to summarize in a consistent H-function notation the integral results required here.

In the subsequent equations, we shall write the symbol $\mathbf{B}$ to denote an arbitrary two-vector with constant elements, B_1 and B_2, and we shall make use of the definitions

$$\alpha_1 = \sigma c_{21} \int_0^{1/\sigma} H(\mu)\mu \, d\mu, \qquad \alpha_2 = c_{22} \int_0^1 H(\mu)\mu \, d\mu, \tag{A-1a, b}$$

$$\alpha = \int_0^1 H(\mu)\Psi(\mu)\mu \, d\mu = \left[\frac{2}{3}\left(\frac{1}{\sigma^2}c_{12} + c_{22}\right)\right]^{1/2}, \tag{A-2}$$

and

$$\tau_* = \frac{1}{\alpha}\int_0^1 H(\mu)\Psi(\mu)\mu^2 \, d\mu; \tag{A-3}$$

here τ_* is the Milne-problem extrapolation distance tabulated by BOND and SIEWERT.[3] Recalling the definition

$$[\mathbf{X}(\mu), \mathbf{Y}(\mu)] = \int_0^1 \tilde{\mathbf{X}}^{\dagger}(\mu)\mathbf{H}(\mu)\mathbf{Y}(\mu) \, d\mu, \tag{A-4}$$

we find

$$[\mathbf{I}_+, \mathbf{B}] = \alpha_1 B_1 + \alpha_2 B_2, \tag{A-5}$$

$$[\mathbf{I}_+, \mathbf{I}_-(\tau, \pm\mu)] = c_{22}\alpha(\tau \mp \tau_*), \tag{A-6}$$

$$[\mathbf{I}_+, \mathbf{\Phi}(-\eta', \mu)] = c_{22}\eta'\frac{1}{H(\eta')}, \qquad \eta' \in (0, 1), \tag{A-7}$$

$$[\mathbf{\Phi}_1(\eta, \mu), \mathbf{B}] = D_{11}(\eta)B_1 + D_{12}(\eta)B_2, \qquad \eta \in (0, 1/\sigma), \tag{A-8}$$

$$[\mathbf{\Phi}_1(\eta, \mu), \mathbf{I}_-(\tau, \pm\mu)] = \pm c_{22}\eta\alpha M_{12}(\eta), \qquad \eta \in (0, 1/\sigma), \tag{A-9}$$

$$[\mathbf{\Phi}_1(\eta, \mu), \mathbf{\Phi}(-\eta', \mu)] = c_{22}\eta\eta'\frac{1}{H(\eta')(\eta' + \eta)}M_{12}(\eta), \qquad \eta \in (0, 1/\sigma), \eta' \in (0, 1), \tag{A-10}$$

$$[\mathbf{\Phi}(\eta, \mu), \mathbf{B}] = D_1(\eta)B_1 + D_2(\eta)B_2, \qquad \eta \in (0, 1), \tag{A-11}$$

$$[\mathbf{\Phi}(\eta, \mu), \mathbf{I}_-(\tau, \pm\mu)] = \pm\eta\alpha\Psi(\eta), \qquad \eta \in (0, 1), \tag{A-12}$$

and

$$[\mathbf{\Phi}(\eta, \mu), \mathbf{\Phi}(-\eta', \mu)] = \eta\eta' \frac{1}{H(\eta')(\eta' + \eta)} \Psi(\eta), \qquad \eta, \eta' \in (0, 1). \tag{A-13}$$

We note that the identity

$$P \int_0^1 H(\mu)\Psi(\mu)\mu \frac{d\mu}{\mu - \eta} = H(\eta)\left[1 - 2\eta c_{22}\mathscr{T}(\eta) - 2\eta c_{11}\left\{\mathscr{T}(\sigma\eta)\Theta(\eta) + \mathscr{T}\left(\frac{1}{\sigma\eta}\right)[1 - \Theta(\eta)]\right\}\right] \tag{A-14}$$

is required to establish several of the foregoing results. In addition, we have made use of the previous[3] definitions

$$M_{11}(\eta) = \frac{1}{c_{11}c_{22}}\{c_{22}(c_{11} + c_{22})\pi^2\eta^2 + [1 - 2\eta c_{22}\mathscr{T}(\eta)]^2 + 4\eta^2 c_{11}c_{22}\mathscr{T}^2(\sigma\eta)\}, \tag{A-15a}$$

$$M_{22}(\eta) = \frac{1}{c_{22}}(c_{11} + c_{22}), \tag{A-15b}$$

and

$$M_{21}(\eta) = M_{12}(\eta) = \frac{1}{c_{22}}[1 - 2\eta c_{22}\mathscr{T}(\eta) + 2\eta c_{22}\mathscr{T}(\sigma\eta)], \tag{A-15c}$$

and have introduced the quantities

$$D_{11}(\eta) = \sigma c_{21}\eta\left\{H(\eta)[M_{11}(\eta) - 2\eta\mathscr{T}(\sigma\eta)M_{12}(\eta)] - M_{12}(\eta)P\int_0^{1/\sigma} H(\mu)\mu\frac{d\mu}{\mu - \eta}\right\}, \tag{A-16a}$$

$$D_{12}(\eta) = \eta H(\eta)\{-c_{11}M_{11}(\eta) + [1 - 2\eta c_{22}\mathscr{T}(\eta)]M_{12}(\eta)\} - M_{12}(\eta)c_{22}\eta P\int_0^1 H(\mu)\mu\frac{d\mu}{\mu - \eta}, \tag{A-16b}$$

$$D_1(\eta) = \sigma c_{21}\eta\left\{H(\eta)[M_{21}(\eta) - 2M_{22}(\eta)\eta\mathscr{T}(\sigma\eta)]\Theta(\eta) - \frac{1}{c_{22}}\Psi(\eta)P\int_0^{1/\sigma} H(\mu)\mu\frac{d\mu}{\mu - \eta}\right\}, \tag{A-16c}$$

and

$$D_2(\eta) = \eta H(\eta)\left\{-c_{11}M_{21}(\eta)\Theta(\eta) - 2\eta c_{11}\mathscr{T}\left(\frac{1}{\sigma\eta}\right)[1 - \Theta(\eta)] + \frac{1}{c_{22}}\Psi(\eta)[1 - 2\eta c_{22}\mathscr{T}(\eta)]\right\} - \Psi(\eta)\eta P\int_0^1 H(\mu)\mu\frac{d\mu}{\mu - \eta}. \tag{A-16d}$$

APPENDIX B

To complete this work, we should like to define the various known matrices appearing in equations (30). First, on the left-hand sides of those equations, we find

$$\mathbf{S} = -\alpha_1\mathbf{K}_1 - \alpha_2\mathbf{K}_2 - \alpha c_{22}\begin{vmatrix}\rho_1^s - 1 & \tau_*(\rho_1^s + 1)\\ \rho_2^s - 1 & \tau_0(\rho_2^s - 1) - \tau_*(\rho_2^s + 1)\end{vmatrix}, \tag{B-1}$$

where

$$\mathbf{K}_i = \frac{w_i}{2(\sigma w_1 + w_2)}\begin{vmatrix}\rho_{1i}^d & \rho_{1i}^d\frac{2}{3}\frac{c_{12}}{c_{1i}}\\ \rho_{2i}^d & \rho_{2i}^d\left(\tau_0 - \frac{2}{3}\frac{c_{12}}{c_{1i}}\right)\end{vmatrix}, \quad i = 1 \text{ and } 2, \tag{B-2}$$

$$\mathbf{S}_1(\eta) = \eta H(\eta)N_1(\eta)\mathcal{M}(\eta) \text{ and } \mathbf{S}(\eta) = \eta H(\eta)N(\eta)\mathcal{M}(\eta), \tag{B-3}$$

where

$$\mathcal{M}(\eta) = \begin{vmatrix}1 & -\rho_1^s\\ -\rho_2^s\,e^{-\tau_0/\eta} & e^{\tau_0/\eta}\end{vmatrix}. \tag{B-4}$$

The free terms on the right-hand sides of equations (30) can be written as

$$\mathbf{G} = |\mathbf{A}_1 \quad \mathbf{A}_2|^T\boldsymbol{\alpha}, \tag{B-5a}$$

$$\mathbf{G}_1(\eta) = |\mathbf{A}_1 \quad \mathbf{A}_2|^T\mathbf{D}_1(\eta) \text{ and } \mathbf{G}(\eta) = |\mathbf{A}_1 \quad \mathbf{A}_2|^T\mathbf{D}(\eta), \tag{B-5b, c}$$

where $\boldsymbol{\alpha}$, $\mathbf{D}_1(\eta)$ and $\mathbf{D}(\eta)$ are column vectors with elements α_1 and α_2, $D_{11}(\eta)$ and $D_{12}(\eta)$, and $D_1(\eta)$ and $D_2(\eta)$ respectively.

In addition, we have made the definitions

$$\mathbf{W}_1(\eta) = D_{11}(\eta)\mathbf{K}_1 + D_{12}(\eta)\mathbf{K}_2 + \alpha\eta c_{22}M_{12}(\eta)\begin{vmatrix}0 & -1 - \rho_1^s\\ 0 & 1 + \rho_2^s\end{vmatrix}, \tag{B-6}$$

$$\mathbf{W}(\eta) = D_1(\eta)\mathbf{K}_1 + D_2(\eta)\mathbf{K}_2 + \alpha\eta\Psi(\eta)\begin{vmatrix}0 & -1 - \rho_1^s\\ 0 & 1 + \rho_2^s\end{vmatrix}, \tag{B-7}$$

$$\mathbf{U}(\eta) = \alpha_1\mathbf{E}_{11}(\eta) + \alpha_2\mathbf{E}_{12}(\eta), \tag{B-8}$$

and

$$\mathbf{V}(\eta) = \alpha_1\mathbf{E}_1(\eta) + \alpha_2\mathbf{E}_2(\eta) + c_{22}\eta\frac{1}{H(\eta)}\mathbf{B}(\eta), \tag{B-9}$$

where

$$\mathbf{B}(\eta) = \begin{vmatrix}\rho_1^s & -1\\ -e^{-\tau_0/\eta} & \rho_2^s\,e^{\tau_0/\eta}\end{vmatrix}, \tag{B-10}$$

$$\mathbf{E}_{1j}(\eta) = 2\begin{vmatrix}\rho_{1j}^d J_{1j}(\eta) & \rho_{1j}^d J_{1j}(-\eta)\\ \rho_{2j}^d J_{1j}(-\eta)\,e^{-\tau_0/\eta} & \rho_{2j}^d J_{1j}(\eta)\,e^{\tau_0/\eta}\end{vmatrix}, \tag{B-11}$$

and

$$\mathbf{E}_j(\eta) = 2\begin{vmatrix} \rho^d_{1j} J_j(\eta) & \rho^d_{1j} J_j(-\eta) \\ \rho^d_{2j} J_j(-\eta)\, e^{-\tau_0/\eta} & \rho^d_{2j} J_j(\eta)\, e^{\tau_0/\eta} \end{vmatrix}. \tag{B-12}$$

Finally, we note that

$$\mathbf{U}_1(\eta, \eta') = D_{11}(\eta')\mathbf{E}_{11}(\eta) + D_{12}(\eta')\mathbf{E}_{12}(\eta), \tag{B-13}$$

$$\mathbf{U}(\eta, \eta') = D_1(\eta')\mathbf{E}_{11}(\eta) + D_2(\eta')\mathbf{E}_{12}(\eta), \tag{B-14}$$

$$\mathbf{V}_1(\eta, \eta') = D_{11}(\eta')\mathbf{E}_1(\eta) + D_{12}(\eta')\mathbf{E}_2(\eta) + c_{22}\eta\eta' \frac{1}{H(\eta)(\eta + \eta')} M_{12}(\eta')\mathbf{B}(\eta), \tag{B-15}$$

and

$$\mathbf{V}(\eta, \eta') = D_1(\eta')\mathbf{E}_1(\eta) + D_2(\eta')\mathbf{E}_2(\eta) + \eta\eta'\Psi(\eta') \frac{1}{H(\eta)(\eta + \eta')} \mathbf{B}(\eta). \tag{B-16}$$